


# Modeling vegetation dynamics under climate change in wetlands of Taza province using remote sensing and machine learning

Hazyoun Zineb<sup>1\*</sup> , El Haouari Mohammed<sup>1,2</sup>, Afquir Youssef<sup>3</sup>,  
Assaadi Abdellah<sup>3</sup>, Ben Laghlagh Oumaima<sup>4</sup>, Assem Najat<sup>1,5</sup>

<sup>1</sup> Department of Biology, Laboratory of Biotechnology, Conservation and Valorization of Bioresources (BCVB), Faculty of Sciences Dhar El Mahraz, Sidi Mohamed Ben Abdellah University, Fez 35000, Morocco

<sup>2</sup> Regional Center for Education Careers and Training (CRMEF Fès-Meknès), Taza 35000 Morocco

<sup>3</sup> Laboratory of Ecology and Environment, Faculty of Sciences Ben M'sik, Hassan II University in Casablanca, Av. Cdt Driss El Harti, BP 7955, Sidi Othman, 20000 Casablanca, Morocco

<sup>4</sup> Geo-Resources and environment Laboratory, Faculty of Sciences and Technology of Fez, Sidi Mohammed Ben Abdellah University, BP. 2202, Fez, Morocco

<sup>5</sup> Polydisciplinary Faculty of Taza, Sidi Mohamed Ben Abdellah University, Fez 35000, Morocco

\* Corresponding author's e-mail: Zineb.hazyoun@usmba.ac.ma

## ABSTRACT

The wetlands of the province of Taza (Morocco) are highly sensitive to climate variability due to pronounced spatial heterogeneity, with arid plains and wetter high-altitude areas. This study investigates the spatio-temporal dynamics of vegetation cover in these wetlands and predicts future changes under climate change scenarios using an integrated approach that combines remote sensing (NDVI) and machine learning algorithms (MaxEnt, Random Forest, and XGBoost). A set of bioclimatic, topographic, and hydrological variables was used to model vegetation distribution, and model performance was evaluated using AUC metrics. Results indicate that XGBoost and Random Forest outperform MaxEnt, providing highly accurate predictions of vegetation dynamics. Current NDVI patterns show that low-density vegetation dominates approximately 42% of the study area, while medium and high NDVI classes cover 33% and 26%, respectively. Projections to 2060 and 2100 under SSP 245 and SSP 585 scenarios suggest a slight decline in low NDVI areas, relative stability of medium NDVI classes, and moderate expansion of high NDVI areas, indicating resilience in some ecosystems. Spatial analysis further identifies specific stations (Oued El Bared, Lac Tamda, Oued M'soun, and Oued Chaouya) as highly vulnerable to combined climate and anthropogenic pressures, whereas others (Bab Louta and Ras El Ma) show greater resilience. This study demonstrates that integrating NDVI with machine learning enables robust prediction of vegetation responses to climate change, providing a scientific basis for adaptive management and conservation strategies in vulnerable wetland ecosystems.

**Keywords:** wetlands, province of Taza, climate change, NDVI, machine learning.

## INTRODUCTION

Climate change is widely recognized as one of the major drivers affecting terrestrial ecosystems worldwide. Changes in temperature, precipitation patterns, and the increasing frequency of extreme climatic events can significantly alter vegetation dynamics, ecosystem productivity, and biodiversity. Vegetation plays a key role in

regulating ecological processes such as carbon sequestration, water balance, and habitat provision, making it particularly sensitive to climatic variability. Consequently, understanding how vegetation responds to climate change has become an important focus in ecological research, particularly in regions where ecosystems are already exposed to climatic stress and environmental degradation.

In this context, climate change represents an additional threat to plant and animal populations (Sala et al., 2001). Its impacts on vegetation dynamics may lead to significant disturbances in terrestrial ecosystems, including reductions in biodiversity and ecosystem resilience. As a result, assessing ecosystem vulnerability has become a central topic in ecological research (Reichstein et al., 2013; Zhou et al., 2014; Xu et al., 2020).

To better understand these processes and monitor vegetation responses to environmental change, remote sensing has become an essential tool for analyzing vegetation dynamics over large spatial and temporal scales. Satellite imagery allows continuous observation of vegetation conditions and provides valuable information on ecosystem responses to environmental changes. Among the most widely used indicators, the normalized difference vegetation index (NDVI) is commonly applied to assess vegetation vigor, density, and productivity based on the spectral response of plant canopies. NDVI derived from satellite platforms such as the Landsat program and Sentinel-2 has been extensively used to analyze long-term trends in vegetation cover, detect land degradation processes, and evaluate ecosystem responses to climate variability across different environmental contexts.

Vegetation dynamics are influenced by several environmental parameters, particularly climatic and hydrological factors that control ecosystem water balance. Changes in precipitation and temperature can modify processes such as evapotranspiration, interception, and soil moisture availability, thereby influencing vegetation growth and distribution (Singh et al., 2003; Orimoloye et al., 2018). The consequences of these interactions may lead to vegetation degradation and biodiversity loss across different ecological environments (Germer et al., 2011).

In North Africa, and particularly in Morocco, ecosystems are increasingly affected by climate variability and long-term climatic changes. The Kingdom of Morocco is considered one of the African countries most vulnerable to climate change and its associated impacts. Long-term climatic observations indicate a clear warming trend accompanied by decreasing rainfall and an increasing frequency of extreme weather events (Chaqdid et al., 2023; Ait Brahim et al., 2023). According to Driouech et al. (2021), the average annual temperature increased by approximately 1.1 °C per decade between 1984 and 2016 across

the country. In addition, several studies have reported significant changes in the timing and spatial distribution of precipitation (Tramblay et al., 2012; Abahous et al., 2018; Bouizrou et al., 2022). In southern regions of Morocco, rainfall has decreased by approximately 27–37 mm per decade between 1970 and 2012. Overall, precipitation variability ranges between 50 and 80%, while maximum daily temperatures have increased by about 1.5 °C since 1900, with important environmental consequences (IPCC, 2022).

Given these climatic pressures, effective adaptation and management strategies are increasingly required to mitigate the impacts of climate change on agricultural and forest ecosystems. Such strategies often involve collaboration among different stakeholders and require reliable scientific information to support decision-making processes (Eckardt et al., 2023; Godde et al., 2020). Consequently, modeling and prediction tools have become essential for assessing future ecological changes and supporting sustainable resource management.

In recent years, modeling approaches based on Machine Learning have increasingly been used to analyze and predict vegetation distribution and ecosystem responses to environmental change. These algorithms are capable of capturing complex and non-linear relationships between vegetation patterns and environmental variables such as climate, topography, and hydrological conditions. Several methods have been widely applied in ecological modeling, including Maximum Entropy Modeling (MaxEnt), Random Forest, and XGBoost. These approaches have demonstrated strong predictive performance in studies related to habitat suitability, land-use change, and vegetation dynamics, making them valuable tools for assessing potential ecological responses to future climate scenarios.

More specifically, predictive models have been widely used to simulate species distribution and vegetation suitability under different environmental conditions (Garzón et al., 2006; Keenan et al., 2011; Blanco et al., 2020). These models generate spatially explicit maps that represent habitat suitability or potential vegetation distribution (Elith et al., 2006; Tarkesh and Jetschke, 2012; Bedair et al., 2023). Over the past decades, predictive vegetation modeling has progressively shifted toward machine learning approaches, which provide improved accuracy and flexibility in ecological applications (Almeida et al., 2023; Beigaité et al., 2022; Ferchichi et al., 2022; Qu et

al., 2024). These algorithms have been successfully applied in several environmental studies, including fire risk mapping, hydrogeological hazard assessment, and land-use change prediction (Javidan et al., 2021; Martín et al., 2019; Norallah et al., 2021; Kavhu et al., 2021).

Within Morocco, the province of Taza represents a particularly sensitive region due to its climatic contrasts, characterized by relatively arid plains and higher rainfall in mountainous areas. These environmental gradients create diverse ecosystems that are vulnerable to climatic variability. Recent studies have reported a decline in floral diversity, habitat degradation, and increased vulnerability of vegetation cover to climate variability in this region (El Madihi et al., 2021; Hazyoum et al., 2025). These findings highlight the importance of developing robust approaches to anticipate future ecological changes and support sustainable ecosystem management.

Despite the growing application of remote sensing and predictive modeling in ecological research, spatio-temporal analyses of vegetation dynamics remain limited in many semi-arid Mediterranean regions, including Taza Province. Wetlands located in climatically heterogeneous landscapes are particularly understudied, even though they represent ecosystems highly sensitive to climatic variability and anthropogenic pressures. Most previous studies in Morocco have focused primarily on regional climate trends or biodiversity inventories, while fewer investigations have integrated satellite-derived vegetation indices with predictive modeling approaches to assess vegetation responses to climate change at the local scale. This lack of integrated analyses limits the ability to anticipate future vegetation changes and to support effective ecosystem conservation and management.

To address this research gap, the present study aims to analyze the spatio-temporal evolution of vegetation cover in the wetlands of Taza Province using satellite-derived NDVI time series. Furthermore, machine learning algorithms, including MaxEnt, Random Forest, and XGBoost, are applied to model and predict future vegetation dynamics under different climate change scenarios. The objectives of this study are to (i) evaluate the predictive performance of these models, (ii) identify vulnerable and resilient wetland ecosystems, and (iii) provide projections of vegetation changes under mid- and long-term climate scenarios to support adaptation and conservation strategies.

## MATERIALS AND METHODS

### Study areas

Our study was conducted in the province of Taza (Figure 1), which covers an area of 7.101 km<sup>2</sup> and is characterized by its mountainous terrain. It is divided into the Rif and Atlas regions, representing the meeting point between the Rif and the Middle Atlas.

The study area is located between two different geological domains: the Middle Atlas and the Pre-Rifain sector. This area offers the character of a contrasting mountain region with plateaus, hills, and plains. Thus, the study area extends over two different structural domains of Morocco, namely the Meseto-Atlas domain and the Rif domain. In addition, the region is characterized by fairly high altitudes (1.500 to 2.000 m in the Tazekka but-tonhole region), which allows for winter rainfall (more than 1.000 mm/year on average).

The province of Taza is bordered to the north by the province of Al-Hoceima, to the northeast by Nador, to the east by Taourirt, to the south by Boulemane, and to the west by the provinces of Taounate and Sefrou (latitude: 34° 13' 00" N, longitude: 4° 01' 00" W, altitude: 550 m).

Eight study stations were carefully selected (Figure 1) in the province of Taza, namely:

- Oued M'Soun and Oued Chaouya, located in the municipality of Aknoul;
- Ras El Ma (Ras-El-Oued), located south of the city of Taza, in the municipality of Bab Boudir;
- Oued El Bared, which belongs to the municipality of Maghraoua;
- Lake Tamda (Guelta Tamda), which is a natural lake in the rural municipality of Bouiblanc;
- Bab Louta, which is located in the municipality of Smiaa;
- Oued Marticha, which is located in the municipality of El Gouzat; and finally Oued Lhajar, which is located in the municipality of Tainaste.

### Climate data

Information on annual precipitation and temperature was obtained from the National Agency for Water and Forests, Taza provincial office. These observations were used to build the ombrothermic diagram describing the climatic regime of the study area.

Recent climate data used in this study were obtained from the WorldClim v2.1 database

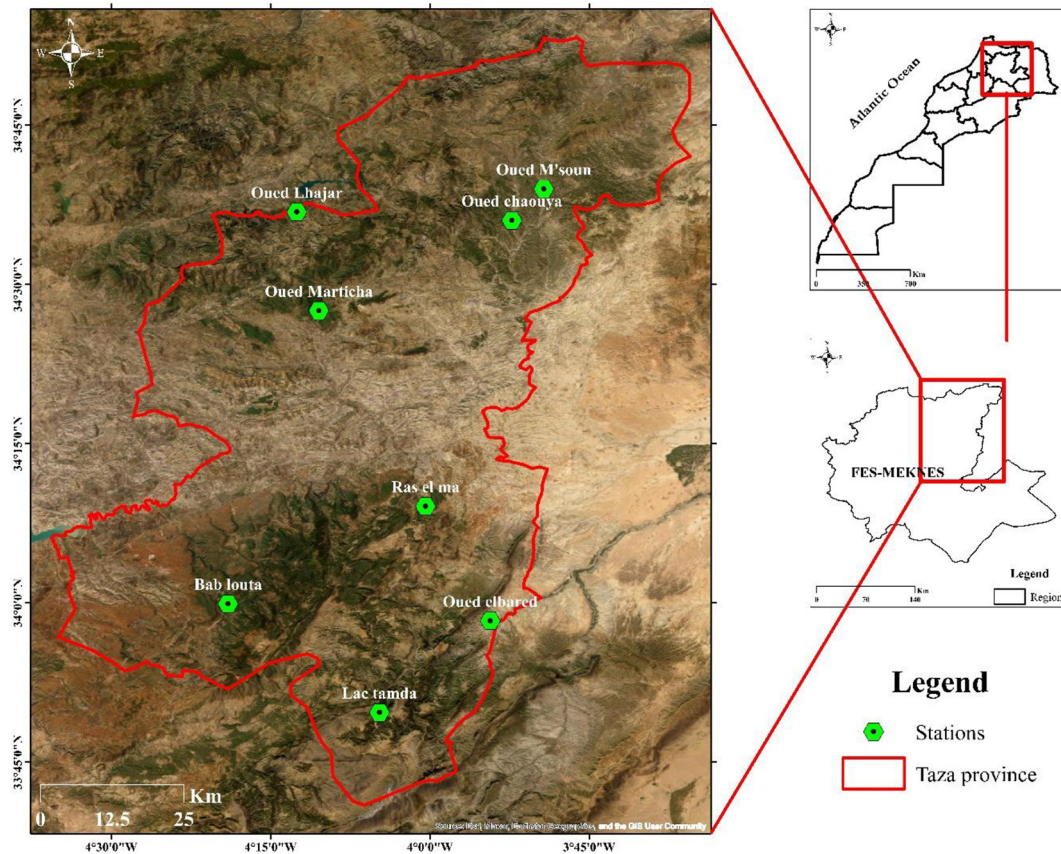


**Figure 1.** Spatial distribution of study areas in the province of Taza

(Fick and Hijmans, 2017), which provides interpolated climate surfaces representing the reference period 1970–2000 at a spatial resolution of 2.5 arc-minutes (~5 km). Selected bioclimatic variables included temperature and precipitation-related indicators commonly used in ecological modelling.

Future climate projections were derived from the ACCESS-CM2, one of the global climate models developed within the CMIP6 framework using the WorldClim v2.1 database with the same resolution of the historic data. The ACCESS-CM2 model was developed by the Commonwealth Scientific and Industrial Research Organisation (CSIRO) and has been widely used in climate projection studies (Dix et al., 2019).

Two shared socioeconomic pathway (SSP) scenarios were selected to represent different greenhouse gas emission trajectories SSP 245, representing a moderate or intermediate emission pathway and SSP 585, representing a high-emission or pessimistic scenario. We use two-time horizons: 2060, and 2100, allowing the assessment of potential climate impacts on vegetation dynamics in the study area.

### Vegetation data

Vegetation maps were developed based on the period of maximum photosynthesis observed in the analyzed region. Sentinel-2 Level 2A surface reflectance images were used to obtain vegetation data, thanks to their high spatial resolution (10 m for B2, B3, B4, and B8) and their relevance for vegetation monitoring. Initially, a vector file of the Taza area was developed using QGIS v3.40.0, before being transferred to the Google Earth Engine (GEE) platform. The selection of Sentinel-2 images (COPERNICUS/S2\_SR) was made to focus exclusively on the target area and the spring season from March 1 to April 20, 2025, retaining only scenes with less than 10% cloud cover in the WGS84 coordinate system. A median composition was produced to minimize contamination from clouds and temporal fluctuations. The standard equation was then used to calculate the normalized difference vegetation index (NDVI), which is a standard index (Rouse and Haas, 1973; Tucker, 1979) used for vegetation analysis (Gao, 1996). It is calculated from the red (R) and near-infrared (NIR) spectral bands. This index, normalized

between -1 and +1, distinguishes non-vegetated surfaces, such as water (-1), from areas of active vegetation (+1). The NDVI formula is as follows:

$$NDVI = \frac{NIR - R}{NIR + R} \quad (1)$$

where: *NIR* – reflectance in the near infrared band, *R* – reflectance in the red band.

The NDVI map obtained was then classified into three classes (low, medium, and high) using unsupervised K-means classification in the platform GEE, corresponding to increasing levels of vegetation density and photosynthetic activity. These classes were used as the target variable for modeling.

Several phytoecological surveys were carried out during successive field trips in March 2024, using the plot sampling method with MapsOffline software to determine the location of the plots, thus ensuring adequate spatial representation of the study area. This plot selection rule was developed in order to adequately represent the ecologic variety of the site with a systematic and reproducible procedure that tries to encompass both vegetation cover and species frequency (Braun-Blanquet, 1932).

### Environmental variables

A set of environmental predictors (Table 1) was chosen to investigate vegetation distribution and dynamics, including bioclimatic, topographic, and hydrological variables. Bioclimatic variables, topographic variables (elevation, slope, and exposure) were derived from digital elevation model. Furthermore, the indices include NDWI, which is to observe the characteristics of each land target in several spectral bands and, then, the segmentation of land from open water. Actually, the NDWI index is the reciprocal to NDVI index (McFeeters, 1996 and Xu, 2006). According to Sims and Gamon (2003), the NDWI is an adequate water absorption index compared to the NDVI. Its values range between -1 and +1 (McFeeters, 1996). To characterize surface moisture conditions, the topographic moisture index (TWI) was calculated in Google Earth Engine (GEE). It was created by Beven and Kirkby in 1979. Based on DEM, this index is calculated depending on the slope and drained area, to discern areas where water is stagnant, and, thus, the soil moisture may be higher.

All predictors were resampled to a spatial resolution of 30 meters to align with the NDVI grid using the terra library (v1.9-1; <https://CRAN.R-project.org/package=terra>). Continuous variables were resampled using bilinear interpolation, while categorical variables (soil and land cover) were resampled using the nearest-neighbor method. To address potential collinearity, Pearson's correlation coefficients were calculated between predictors (Table 1). Variables exhibiting high correlation, defined as Pearson's *r* values  $\geq 0.75$  or  $\leq -0.75$ , were identified and subsequently removed following the guidelines of Mecherghi et al. (2021).

For each model type (Random Forest, XGBoost, and MaxEnt), a single balanced training dataset was randomly extracted from the stacked predictors and the NDVI reference raster. This dataset was then used to train all classes within that model type. Specifically, MaxEnt models were trained on a one-vs-rest basis, with one model per class, while sharing the same training points across models. All training datasets were saved to ensure reproducibility.

### Distribution modeling

In this study, vegetation distribution dynamics were modeled using three machine learning algorithms: Random Forest (randomForest v4.7-1.2; <https://CRAN.R-project.org/package=randomForest>), XGBoost (xgboost v3.2.0.1; <https://CRAN.R-project.org/package=xgboost>), and Maximum Entropy (MaxEnt, implemented via the maxnet v0.1.4 package; <https://CRAN.R-project.org/package=maxnet>). Training data were generated through a stratified random sampling approach applied to the NDVI classification map, which was categorized from the start into three vegetation classes: low, medium, and high, alongside the environmental predictors. About 1,000 balanced samples were used to ensure equal representation of each NDVI class. The dataset was split into training (65%) and testing (35%) subsets using a fixed random seed (42) to guarantee reproducibility. To ensure the spatial consistency between the response variable and the observations. After filtering out missing values, each class was represented by 333 points, ensuring a globally balanced dataset.

Random Forest models were trained with 500 trees, and variable importance was evaluated

using the Gini impurity index. XGBoost was configured with a learning rate (eta) of 0.05, a maximum tree depth of 6, 600 boosting rounds, subsample and column sample ratios of 0.8, and early stopping after 30 rounds without improvement. MaxEnt models employed a one-versus-rest approach for multi-class classification, enabling all feature types and using the cloglog output format.

Model predictive performance was evaluated using the area under the ROC curve (AUC), which measures the probability that a randomly selected presence pixel is assigned a higher predicted value than a randomly selected absence pixel. This metric assesses the model’s ability to distinguish presence from absence locations (Elith et al., 2006; Phillips et al., 2006). AUC

values range from 0 to 1, where values  $\geq 0.75$  indicate good performance, values around 0.5 indicate predictive discrimination close to random chance, and values below 0.5 indicate worse than chance performance (Elith et al., 2006).

Spatial predictions were generated over the study area using the predict() function from the terra package, producing probability maps for each vegetation class. Final classification maps were created by assigning each pixel to the class with the highest predicted probability.

To quantify areal changes in the three NDVI vegetation classes (Low, Medium, and High) under current and future climate scenarios, raster data from observed NDVI (2025) and model predictions (Random Forest, XGBoost, and MaxEnt for 2060 and 2100 under SSP2-4.5 and

**Table 1.** List of environmental variables considered as predictors for modeling in the province of Taza

Type (Source)	Code	Description	Units	Status
Climate (WorldClim – historical and future), spatial resolution: $\approx 2.5$ arc-minutes ( $\sim 5$ km)	Bio1	Annual mean temperature	$^{\circ}\text{C}$	Discarded
	Bio 2	Mean diurnal range (mean of monthly max–min temperature)	$^{\circ}\text{C}$	Retained
	Bio3	Isothermality (BIO2/BIO7 $\times$ 100)	$^{\circ}\text{C}$	Retained
	Bio4	Temperature seasonality (standard deviation $\times$ 100)	$^{\circ}\text{C}$	Discarded
	Bio5	Maximum temperature of warmest month	$^{\circ}\text{C}$	Retained
	Bio 6	Minimum temperature of coldest month	$^{\circ}\text{C}$	Discarded
	Bio 7	Temperature annual range (BIO5 – BIO6)	$^{\circ}\text{C}$	Retained
	Bio 8	Mean temperature of wettest quarter	$^{\circ}\text{C}$	Retained
	Bio 9	Mean temperature of driest quarter	$^{\circ}\text{C}$	Discarded
	Bio 10	Mean temperature of warmest quarter	$^{\circ}\text{C}$	Discarded
	Bio 11	Mean temperature of coldest quarter	$^{\circ}\text{C}$	Discarded
	Bio 12	Annual precipitation	mm	Retained
	Bio 13	Precipitation of wettest month	mm	Discarded
	Bio14	Precipitation of driest month	mm	Discarded
	Bio15	Precipitation seasonality (coefficient of variation)	%	Discarded
	Bio16	Precipitation of wettest quarter	mm	Discarded
	Bio17	Precipitation of driest quarter	mm	Discarded
	Bio18	Precipitation of warmest quarter	mm	Retained
	Bio19	Precipitation of coldest quarter	mm	Discarded
Topography, spatial resolution: $\approx 30$ m	Elevation	Terrain elevation above sea level	m	Retained
	Aspect	Slope orientation from North	$^{\circ}$	Retained
	Slope	Steepness of the land surface	$^{\circ}$	Retained
	NDWI	Normalized difference water index		Retained
	DEM	Digital elevation model	m	Retained
	Soil	Integrated soil properties (texture and physicochemical characteristics)		Retained
	LandSurf	Land surface characteristics / land cover information		Retained

SSP5-8.5 scenarios). For each raster, the surface area of each class was calculated by multiplying the number of pixels per class by the cell size. The 2025 NDVI map served as a baseline, with class areas replicated for each model and scenario to enable comparisons. Class identifiers were replaced with descriptive labels (Low, Medium, High), and datasets were combined into a unified table. Changes in surface area relative to the 2025 baseline were then computed, for each vegetation class, model, scenario, and year. In this work the majority of all analyses were conducted in R/RStudio (version 2025-10-31 Build 452).

## RESULTS

### Climatic data

An examination of the ombrothermic diagrams (Figure 2) for stations in the province of Taza reveals a Mediterranean climate characterized by significant spatial heterogeneity. The Guelta Tamda and Oued El Bared stations have a high number of dry months throughout the year, indicating a permanent water deficit, even though the wet season is relatively more pronounced in the cold season. The stations of Bab Louta, Oued Lhajar, and Oued Marticha show more pronounced seasonal variation, with wet months concentrated mainly from October to April, while dry months are concentrated from May to September. The Oued M'Soun, Chaouya, and Ras El Ma stations stand out during the dry period from June to April in the province of Taza. The ombrothermic diagrams for the various stations show a prevalence of dry conditions in the summer, and while winter precipitation is most conducive to recharge, the data from the ombrothermic analyses corroborate Hazyoun et al. (2025), the significant differences in net temperature and rainfall patterns between stations confirm that the climate allows for seasonal variations in vegetation cover dynamics.

### Performance and contribution of variables

In the wetlands of the province of Taza, we observed that the MaxEnt, Random Forest, and XGBoost models showed good overall predictive capabilities. The results highlight that the XGBoost and Random Forest models are by far

the most effective among the algorithms used, with AUC values (Figure 3) for test performance reaching very high values, ranging from 0.97 to 1.00 for each low, medium, and high class. XGBoost stands out for its robustness and indisputable performance, offering a perfect AUC (AUC=1.00) during training and very high values in testing. The Random Forest model also shows interesting performance, although slightly less so in testing, particularly for the intermediate class, while MaxEnt performs less well, with lower and more heterogeneous test AUCs, especially for the intermediate class, due to poorer generalization in the study area. Despite this, we will entrust our spatial prediction to the XGBoost model, followed by Random Forest, then MaxEnt, which performs less well in our study area.

### Assessment of temporal and spatial change in NDVI using the XGBoost model in wetlands in the province of Taza

The results provided by the XGBoost model are an indicator of significant changes in vegetation cover (as a proportion of surface area or absolute surface area (expressed in m<sup>2</sup>)) of the different ecotypes in the assessed territory, comparing the current state (2025) with the projected horizons of 2060 and 2100 (Figure 4), in the climate change scenarios present in the model (SSP245 and SSP585).

### Low NDVI class (discontinuous grasslands, degraded areas)

At present (2025), the low NDVI class (Figure 5) is predominant (0.2503 m<sup>2</sup>), representing 41.88% of the study area and reflecting the high proportion of discontinuous grasslands, partially bare soils, and areas of low plant productivity in the province of Taza. By 2060, this class will be greatly reduced in area. According to SSP245, the area will be equal to (0.2172 m<sup>2</sup>), i.e., 36.34% of the study area, and according to SSP585 (0.2175 m<sup>2</sup>), i.e., 36.39% of the study area, indicating a spatial decline in degraded environments. By 2100, the share of this class remains almost identical to that of 2060, 36.30% (0.2170 m<sup>2</sup>) according to SSP245 and 36.34% (0.2172 m<sup>2</sup>) according to SSP585, reflecting a slowdown in the dynamics of vegetation cover restoration over time.

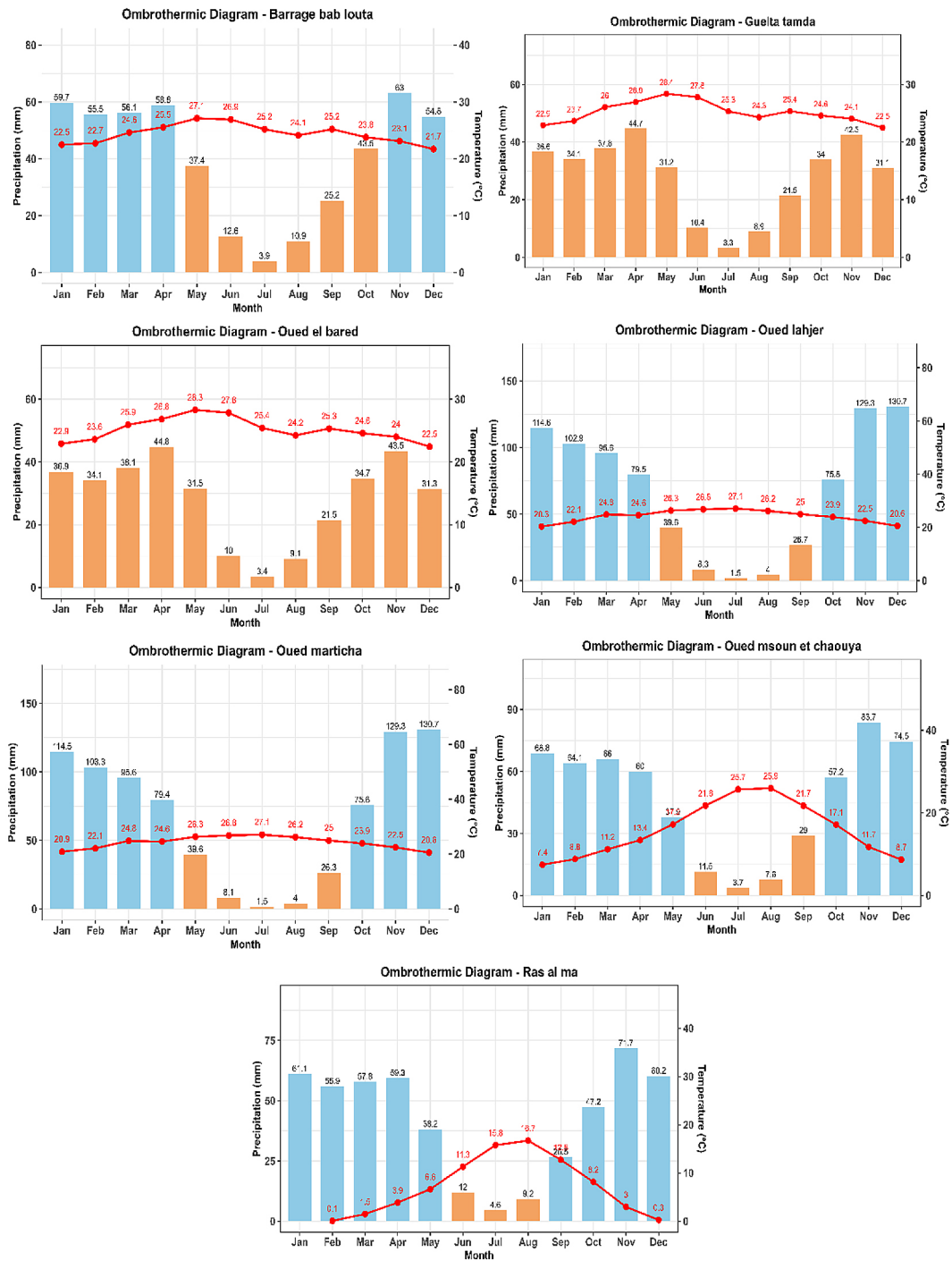


Figure 2. Ombrothermic diagrams for the stations studied in the wetlands of the province of Taza between 1994 and 2024

**Average NDVI class (continuous grasslands and semi-dense formations)**

The average NDVI class (Figure 5) currently (2025) covers 0.1943 m<sup>2</sup> (32.50% of the total area), corresponding to continuous grasslands and intermediate vegetation formations. By 2060, the share of this class will decrease only slightly, with a value of 0.1884 m<sup>2</sup> (31.52%

of the total area) under SSP245 and 0.1883 m<sup>2</sup> (31.49%) under SSP585, reflecting the relative spatial stability of the class. The class shows a slight recovery by 2100, with an area of 0.1896 m<sup>2</sup> (31.72% of the total area) under SSP245 and 0.1893 m<sup>2</sup> (31.67%) under SSP585, confirming the intermediate and buffer role of this class in the face of climate change.

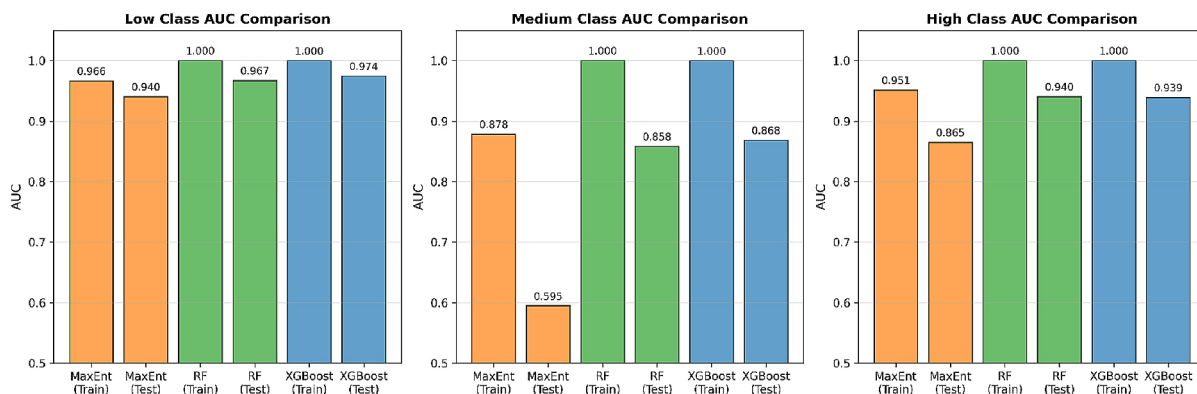


Figure 3. Performance evaluation of the models used according to AUC

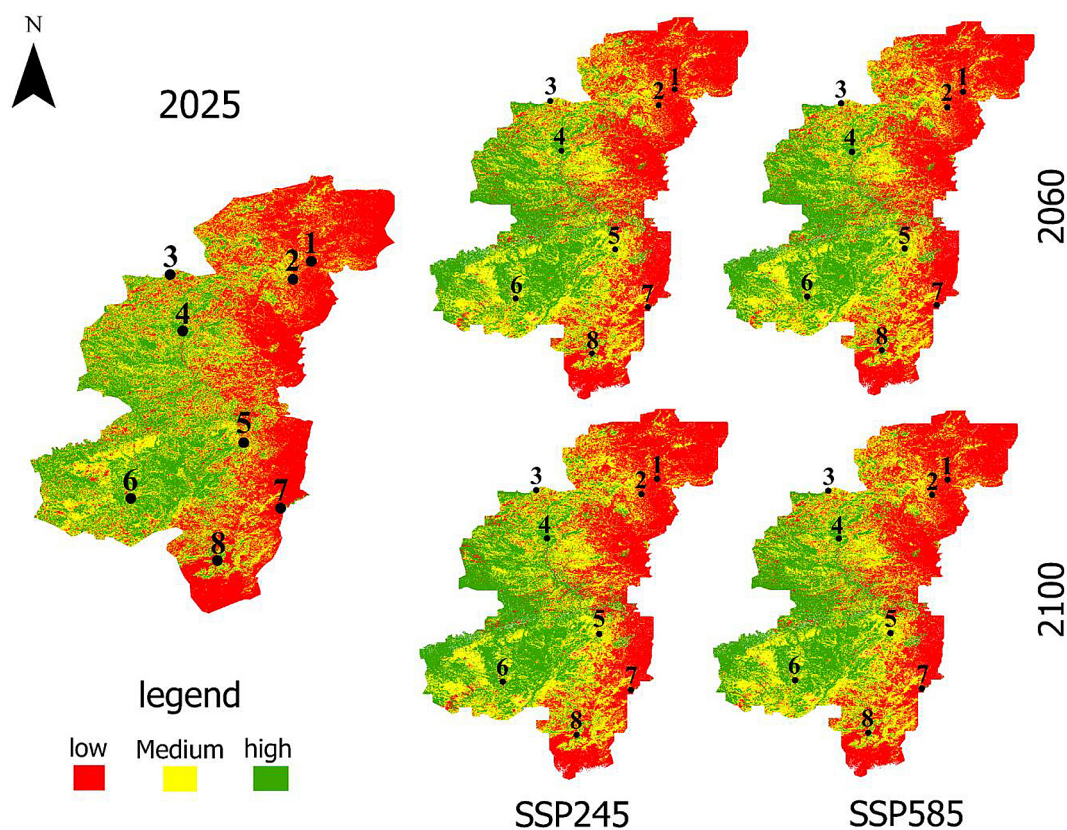


Figure 4. Vegetation changes predicted by XG boost for the study area over three periods (2025, 2060, and 2100) and two climate scenarios (SSP 245 and SSP 585)

### High NDVI classes (forests and dense vegetation)

High NDVI classes (forests and dense vegetation) (Figure 5) represent 0.1532 m<sup>2</sup> (25.62% of the total area) at the present time (2025). By 2060, there will be a slight increase in their spatial area, reaching 0.1634 m<sup>2</sup> (27.34% of the total

area) under SSP245 and 0.1633 m<sup>2</sup> (27.31%) under SSP585, which is sufficient to suggest relative resilience and forest expansion. By 2100, this class remains fairly stable, at 0.1625 m<sup>2</sup> (27.18% of the total area) under SSP245 and 0.1625 m<sup>2</sup> (27.19%) under SSP585, which is enough to suggest a certain long-term vulnerability, at least under the most extreme climate scenarios.

### Environmental degradation in Taza – the most vulnerable stations according to an XGBoost model

The XGBoost analysis carried out on the eight stations in the province of Taza (Oued El Bared, Lake Tamda, Oued Msoun, Oued Chaouya, Oued Lhajar, Oued Marticha, Bab Louta, and Ras El Ma) shows that there is a specific and progressive degradation of environmental quality between the current situation in 2025 and the projections for 2060 and 2100 (Figure 4). In the current situation, the stations at Oued El Bared, Lake Tamda, Oued Msoun, and Oued Chaouya are the most degraded because they are dominated by low classes due to high climate and water pressures, while Oued Lhajar and Oued Marticha are in an intermediate situation with medium classes and moderate vulnerability.

Based on these factors, the localities of Bab Louta and Ras El Ma are characterized by relatively more favorable conditions, notably the relatively larger proportion of middle and upper classes, which effectively gives them a better ecological status compared to the current state of the environment. Medium-term projections indicate a more widespread phenomenon

of degradation for all stations, although the intensity varies greatly depending on the scenario. Thus, according to the SSP245 scenario, degradation continues in a rather gradual manner, leading to an extension well beyond the stations that are already fragile.

In the SSP585 scenario, this differentiation is reinforced, with a rapid and widespread increase in severely degraded areas by 2100. The most vulnerable stations (Oued El Bared, Lak Tamda, Oued Msoun, and Oued Chaouya) are particularly affected, but so are the stations initially classified as the most resilient (Bab Louta and Ras El Ma). Overall, we can deduce from the results obtained that the eight stations are highly sensitive to projected climate change, with greater vulnerability in the eastern and southern parts of the province of Taza, and good performance of the XGBoost model for this type of spatio-temporal approach to environmental degradation, including in a particular configuration of our data.

### Projected changes in vegetation cover in wetlands in the province of Taza through 2100: Comparison of MaxEnt, Random Forest, and XGBoost models

Figure 6 shows the evolution of vegetation in the wetlands of the province of Taza as a percentage of the current state for three dates (2025, 2060, 2100) (Table 2), according to the three projection models (MaxEnt, Random Forest, XGBoost) and the two climate scenarios (SSP245 and SSP585). Major changes can be seen between 2025 and 2060, with areas stabilizing between 2060 and 2100. The MaxEnt model indicates a sharp decline in the low class and an increase in the intermediate class, while the high class declines. Meanwhile, the Random Forest and XGBoost models show much more gradual changes, with a slight decrease in low vegetation areas, relative stagnation in intermediate vegetation, and a slight increase in high vegetation.

For all models, the differences between the two scenarios, SSP245 and SSP585, are very small. This suggests that the results are determined more by the model used than by the climate scenario.

Overall, his projections show the onset of a change in vegetation structure in the wetlands of Taza province towards denser vegetation classes, which appears to be taking place from 2060 onwards.

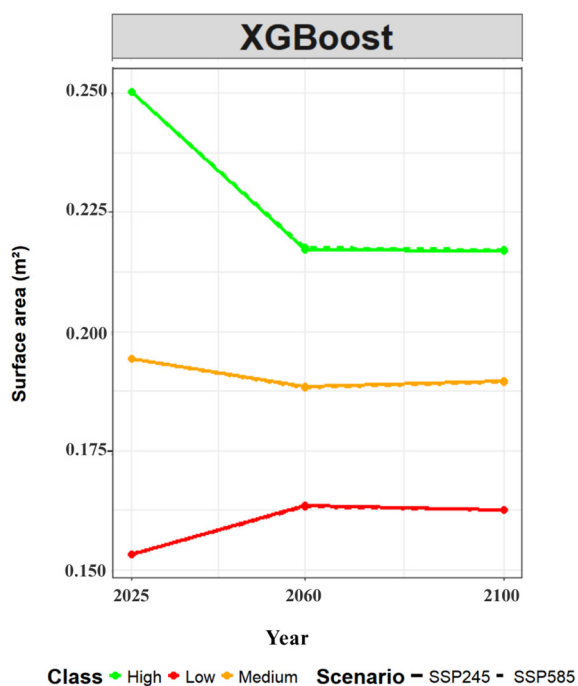


**Figure 5.** Projected vegetation changes in the wetlands of Taza province using the XGBoost model over three periods (2025, 2060, and 2100) and two climate scenarios (SSP 245 and SSP 585)

## DISCUSSION

### Spatio-temporal response of vegetation cover to future climate change in wetlands in the province of Taza

The results of this study suggest a regressive transformation of the vegetation cover structure in the province of Taza under the effect of future climate change. The slight decrease in low NDVI classes and the overall stability, or even slight increase, in medium and high NDVI classes between 2025 and 2060 foreshadow a differentiated response of ecosystems to climatic constraints. Trends observed in several semi-arid regions of Morocco and North Africa where vegetation is limited but not absent, capable of adapting to rising temperatures and precipitation variability (Hazyoun et al., 2025). Nonetheless, the stabilization of the above-mentioned trends by 2100 under the scenario of SSP585 shows a resilience potential but may test the limit of such. Some factors indicate that cumulative impacts of water stress will substantially affect resilience in the long term (Driouech et al. 2021). The degree of climatic variability reflected in the ombrothermic diagrams gives rise to predominantly low NDVI classes found in stations characterised by permanent water deficits, which confirms findings of other studies by Nicholson (2000) and Cherlet et al. (2018), in which water availability limited plant

productivity in semi-arid environments. Finally, NDVI stability does not indicate a fully stable ecological system. It can mask internal changes in vegetation cover, such as changes in the specific composition, density, or physiological state of plants. Studies based on NDVI show that decreased precipitation and increased temperatures lead to a significant decline in photosynthetic activity, particularly in Mediterranean regions where vegetation is already subject to chronic water stress (Anyamba and Tucker, 2012; Fensholt et al., 2015).

A growing body of data indicates a reduction in vegetation cover on a global scale (Almeida et al., 2023; Ben Mariem and Chaieb, 2017; Mechergui et al., 2021; Sarikaya and Orucu, 2021). The increase in patchy grasslands could indicate a shift in this region toward drier conditions, as reported by Sun et al. (2022), who analyzed vegetation patterns as indirect indicators of changes in weather conditions. The expansion of bare soil areas could cause fragmentation and regression of essential habitats as well as a decline in biodiversity, which would have significant impacts on the conservation capacity of protected areas (Bedair et al., 2023; Kaky et al., 2020; Mechergui et al., 2021). The study from the wetlands of the province of Taza provides further evidence of the high degree of sensitivity of vegetation cover to both interannual and future climatic change.

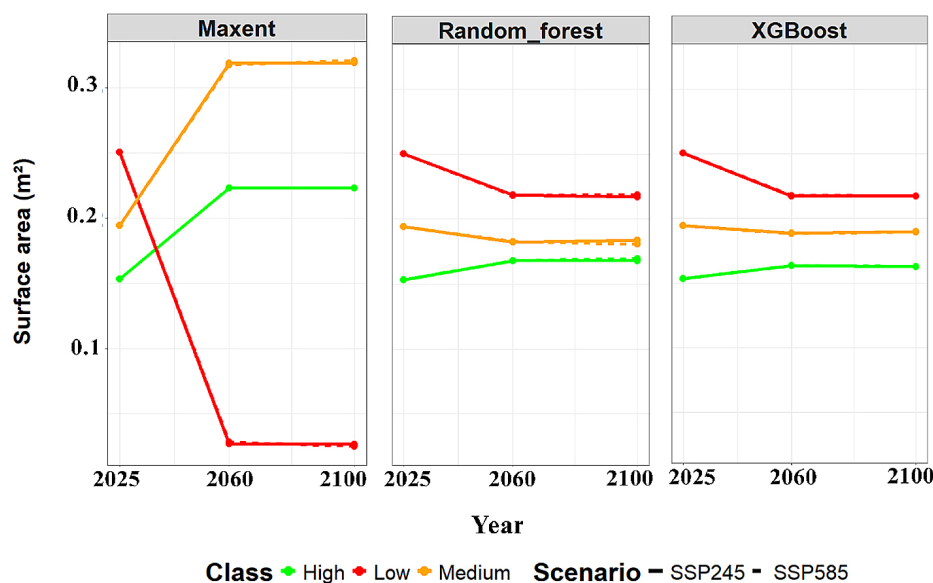


**Figure 6.** Projected vegetation change (in m<sup>2</sup> relative to current conditions) in wetlands in the province of Taza over three periods (2025, 2060, and 2100) according to the three projection models (MaxEnt, Random Forest, and XGBoost) and the two climate scenarios (SSP 245 and SSP 585)

**Table 2.** Area under the receiver operating characteristics curve (AUC) values for the training and test samples for each machine learning algorithm

Model	Classe	AUC_Train	AUC_Test
MaxEnt	Low	0.96	0.94
	Medium	0.87	0.59
	High	0.95	0.86
Random Forest	Low	1	0.96
	Medium	1	0.85
	High	1	0.94
XGBoost	Low	0.99	0.97
	Medium	0.99	0.86
	High	1	0.93

### Effects of human pressure and spatial vulnerability

In various sites, including Oued El Bared, Lac Tamda, and Oued Msoun, the rate of deterioration is much higher than in other locations due to both extreme weather and excessive pressure from people. Several studies have demonstrated that overgrazing, agricultural expansion, and soil degradation are types of human-induced factors that increase the impact of climate change on the growth of vegetation (Le Hou rou, 2001; Geist and Lambin, 2004). Therefore, when these combined types of pressure occur together with prolonged droughts or heat waves, they will hasten the decrease in vegetation coverage and primary production, mainly within the Mediterranean area (Gouveia et al., 2017; Ermit o et al., 2021). On the other hand, the Bab Louta and Ras El Ma stations are better equipped to handle climate change impacts, but the future of these locations will also be impacted by extreme weather, and we anticipate catastrophic events regardless of current vegetation cover condition. These findings are consistent with the IPCC’s (2021) research that stated while the Mediterranean ecosystems are fully adapted to hydrological stress, they will experience escalating risk due to the rising number of extreme meteorological events. The historical adaptation of the Mediterranean ecosystems provides them a level of resistance, but their resilience will fail when the climate disturbance surpasses a certain level.

Based on data confirmed through the use of either Random Forest or XGBoost, many more recent studies have concluded these machine learning techniques are superior to all other methods in their ability to model plant

assemblages, cover types, habitats under climate-related pressures (Elith et al., 2008; Chen and Guestrin and 2016).

It has also been shown that XGBoost improves generalization capacity and robustness in the face of nonlinear interactions between climatic, edaphic, and anthropogenic variables, compared to MaxEnt, in many research contexts (Zhang et al., 2023). Similar discrepancies have also been noted between MaxEnt and tree-based models in other Mediterranean contexts, with MaxEnt also tending to overestimate certain vegetation categories in future climate scenarios (Merow et al., 2013). To determine which areas are most susceptible to climate change impacts and to allocate resources for the conservation/restoration of vegetative cover within the province of Taza, projections for the SSP245 and SSP585 scenarios can be utilized. Therefore, protective measures must be used in order to safeguard forest areas from human activities, thereby allowing ecosystems time to restore and/or return to their original vegetative structures. Over time, it is likely that the ecosystems will achieve a state of balance. The return to an earlier stage of ecological restoration to achieve a more climax-like state recovers ecosystem productivity and resilience and will ensure the sustainable future of these ecosystems as climate change progresses. However, as numerous authors have noted, using NDVI exclusively has very restricted functionality, especially concerning differentiation among plants and ecological status (Pettorelli et al., 2005). Complementary indices will greatly enhance future research; thus it is necessary to have field measurements (specific composition, biomass, functional diversity, water monitoring, soil quality, etc.) included within the study design.

## CONCLUSIONS

This study demonstrates that climate change is likely to exert a differentiated influence on vegetation cover in the wetlands of the province of Taza. Low-density vegetation areas are projected to decrease slightly, while medium and high NDVI classes remain relatively stable or show a modest increase, indicating overall resilience of certain wetland ecosystems.

The XGBoost and Random Forest models outperformed MaxEnt in predictive accuracy, confirming the value of machine learning approaches for modeling complex ecological responses to climate variability. Spatial analysis identified specific stations that are particularly vulnerable to combined climatic and anthropogenic pressures, as well as areas likely to maintain resilience under future climate scenarios.

These findings provide actionable insights for conservation and adaptive management, highlighting where interventions may be most needed to sustain wetland vegetation. The study also establishes a methodological framework for integrating remote sensing, NDVI indices, and machine learning to forecast ecosystem responses under different climate scenarios, addressing a key knowledge gap in regional vegetation dynamics modeling.

## REFERENCES

- Abahous, H., Ronchail, J., Sifeddine, A., Kenny, L., Bouchaou, L. (2018). Trend and change point analyses of annual rainfall in the Souss Massa Region in Morocco during 1932–2010. *Theoretical and Applied Climatology*, 134, 1153–1163. <https://doi.org/10.1007/s00704-017-2325-0>
- Ait Brahim, Y., Sha, L., Wassenburg, J. A., Azenoud, K., Cheng, H., Cruz, F. W., Bouchaou, L. (2023). The spatio-temporal extent of the Green Sahara during the Last Glacial Period. *iScience*, 26, 107018. <https://doi.org/10.1016/j.isci.2023.107018>
- Almeida, A. M., Ribeiro, M. M., Ferreira, M. R., Roque, N., Quintela-Sabaris, C., Fernandez, P. (2023). Big data help to define climate change challenges for the typical Mediterranean species *Cistus ladanifer* L. *Frontiers in Ecology and Evolution*, 11, 1136224. <https://doi.org/10.3389/fevo.2023.1136224>
- Anyamba, A., Tucker, C. J. (2012). Historical perspectives on AVHRR NDVI and vegetation drought monitoring. In B. D. Wardlow et al. (Eds.), *Remote Sensing of Drought: Innovative Monitoring Approaches* (pp. 23–49). CRC Press.
- Bedair, H., Shaltout, K., Halmy, M. W. A. (2023). Stacked machine learning models for predicting species richness and endemism for Mediterranean endemic plants in Egypt. *Plant Ecology*, 224, 1113–1126. <https://doi.org/10.1007/s11258-023-01366-6>
- Beigaitè, R., Tang, H., Bryn, A., et al. (2022). Identifying climate thresholds for dominant natural vegetation types using machine learning. *Global Change Biology*, 28, 3557–3579. <https://doi.org/10.1111/gcb.16110>
- Ben Mariem, H., Chaieb, M. (2017). Climate change impacts on the distribution of *Stipa tenacissima* L. ecosystems in Tunisia. *Applied Ecology and Environmental Research*, 15(3), 67–82.
- Beven, K. J., Kirkby, M. J. (1979). A physically based, variable contributing area model of basin hydrology. *Hydrological Sciences Bulletin*, 24(1), 43–69.
- Blanco, J. A., Ameztegui, A., Rodríguez, F. (2020). Modelling forest ecosystems: a crossroad between scales, techniques and applications. *Ecological Modelling*, 425, 109030.
- Bouizrou, I., Aqnouy, M., Bouadila, A. (2022). Spatio-temporal analysis of rainfall trends across Morocco. *Journal of African Earth Sciences*, 196, 104691.
- Braun-Blanquet, J. 1932. *Plant Sociology: The Study of Plant Communities*. McGraw-Hill.
- Breiman, L. (2001). Random forests. *Machine Learning*, 45(1), 5–32.
- Chen, T., Guestrin, C. (2016). XGBoost: A scalable tree boosting system. *Proceedings of the 22nd ACM SIGKDD Conference*, 785–794.
- Chaquid, A., Tuel, A., El Fatimy, A., El Moçayd, N. (2023). Extreme rainfall events in Morocco: Spatial dependence and climate drivers. *Weather and Climate Extremes*, 40, 100556.
- Cherlet, M., Hutchinson, C., Reynolds, J., et al. (2018). *World Atlas of Desertification*. EU Publications Office.
- Dix, M., Mackallah, C., Bi, D., Bodman, R., Marsland, S., Rashid, H., Woodhouse, M., Druken, K. (2020). CSIRO-ARCCSS ACCESS-CM2 model output prepared for CMIP6 DAMIP. Earth System Grid Federation. <https://doi.org/10.22033/ESGF/CMIP6.14361>
- Driouech, F., Stafi, H., Khouakhi, A., et al. (2021). Recent observed country-wide climate trends in Morocco. *International Journal of Climatology*, 41, 855–874.
- Eckardt, N. A., et al. (2023). Climate change challenges, plant science solutions. *Plant Cell*, 35(1), 24–66.
- El Madihi, M., et al. (2021). Spatio-temporal

- assessment of vegetation cover in Taza region. *Arabian Journal of Geosciences*.
20. Elith, J., Graham, C. H., Anderson, R. P., et al. (2006). Novel methods improve prediction of species' distributions from occurrence data. *Ecography*, 29(2), 129–151.
  21. Elith, J., Leathwick, J. R., Hastie, T. (2008). A working guide to boosted regression trees. *Journal of Animal Ecology*, 77(4), 802–813.
  22. Ermitão, T., Gouveia, C.M., Bastos, A. and Russo, A.C., (2021). Vegetation productivity losses linked to Mediterranean hot and dry events. *Remote Sensing*, 13(19), 4010.
  23. Fensholt, R., et al. (2015). Assessment of vegetation trends in drylands. In: *Remote Sensing Time Series*. Springer.
  24. Ferchichi, A., et al. (2022). Forecasting vegetation indices from spatio-temporal remotely sensed data using deep learning-based approaches: A systematic literature review. *Ecological Informatics*, 68, 101552.
  25. Fick, S. E., and R. J. Hijmans. (2017). WorldClim 2: New 1-km spatial resolution climate surfaces for global land areas. *International Journal of Climatology* 37(12), 4302–4315. <https://doi.org/10.1002/joc.5086>
  26. Gao, B. C. (1996). NDWI – A normalized difference water index for remote sensing of vegetation liquid water from space. *Remote Sensing of Environment*, 58(3), 257–266.
  27. Garzón, M. B., et al. (2006). Predicting habitat suitability with machine learning models: the potential area of *Pinus sylvestris* L. in the Iberian Peninsula. *Ecological Modelling*, 197, 383–393.
  28. Geist, H. J., Lambin, E. F. (2004). Dynamic causal patterns of desertification. *BioScience*, 54(9), 817–829.
  29. Germer, S., Kaiser, K., Bens, O., Hüttl, R. F. (2011). Water balance changes and responses of ecosystems and society in the Berlin-Brandenburg region – a review. *J. Geogr. Soc. Berl.*, 142, 65–95.
  30. Godde, C. M., et al. (2020). Global rangeland production systems and livelihoods at threat under climate change and variability. *Environmental Research Letters*, 15, 044021.
  31. Gouveia, C.M., Trigo, R.M., Beguería, S. and Vicente-Serrano, S.M., 2017. Drought impacts on vegetation activity in the Mediterranean region: An assessment using remote sensing data and multi-scale drought indicators. *Global and Planetary Change*, 151, 15–27.
  32. Hazyoun, Z., Lyazidi, A., Rouai, S., et al. (2025). Impact of climate variability and soil parameters on phytobiodiversity. *Ecological Engineering & Environmental Technology*, 10, 356–370.
  33. IPCC 2021. Climate Change 2021: The Physical Science Basis.
  34. IPCC 2022. Climate Change 2022: Impacts, Adaptation and Vulnerability.
  35. Javidan, N., et al. (2021). Evaluation of multi-hazard map produced using MaxEnt machine learning technique. *Scientific Reports*, 11, 6496.
  36. Kaky, E., Nolan, V., Alatawi, A., Gilbert, F. (2020). A comparison between Ensemble and MaxEnt species distribution modelling approaches for conservation: A case study with Egyptian medicinal plants. *Ecological Informatics*, 60, 101150.
  37. Kavhu, B., Mashimbye, Z. E., Luvuno, L. (2021). Climate-based regionalization and inclusion of spectral indices for enhancing transboundary land-use/cover classification using deep learning and machine learning. *Remote Sensing*, 13, 5054.
  38. Keenan, T., et al. (2011). Predicting the future of forests in the Mediterranean under climate change, with niche- and process-based models: CO<sub>2</sub> matters! *Global Change Biology*, 17(1), 565–579.
  39. Le Houérou, H. N. (2001). Biogeography of the arid steppeland north of the Sahara. *Journal of Arid Environments*, 48(2), 103–128.
  40. Martín, Y., et al. (2019). Modelling temporal variation of fire occurrence towards the dynamic prediction of human wildfire ignition danger in northeast Spain. *Geomatics, Natural Hazards and Risk*, 10(1), 385–411.
  41. McFeeters, S. K. (1996). The use of the Normalized Difference Water Index (NDWI) in the delineation of open water features. *International Journal of Remote Sensing*, 17, 1425–1432.
  42. Mechergui, K., A. S. Altamimi, W. Jaouadi, S. Naghmouchi, and S. El Wellani. (2021). Modelling current and future potential distributions of *Vachellia tortilis* (Forssk.) Hayne Subsp. *Raddiana* (Savi.) Brenan Var. *Raddiana* under climate change in Tunisia. *African Journal of Ecology* 59, 4, 944–958. <https://doi.org/10.1111/aje.12892>
  43. Merow, C., Smith, M. J., Silander, J. A. (2013). Practical guide to MaxEnt for modeling species' distributions: what it does, and why inputs and settings matter. *Ecography*, 36(10), 1058–1069.
  44. Nicholson, S. E., Selato, J. C. (2000). The influence of La Niña on African rainfall. *International Journal of Climatology*, 20, 1761–1776.
  45. Norallahi, M., Seyed Kaboli, H. (2021). Urban flood hazard mapping using machine learning models: GARP, RF, MaxEnt and NB. *Natural Hazards*, 106, 119–137.
  46. Orimoloye, I. R., et al. (2018). Spatiotemporal monitoring of land surface temperature and estimated radiation using remote sensing: human health implications for East London, South Africa. *Environmental Earth Sciences*, 77, 77.

47. Pettorelli, N., et al. (2005). Using the satellite-derived NDVI to assess ecological responses to environmental change. *Trends in Ecology & Evolution*, 20(9), 503–510.
48. Phillips, S. J., Anderson, R. P., Schapire, R. E. (2006). Maximum entropy modeling of species geographic distributions. *Ecological Modelling*, 190, 231–259.
49. Qu, J., Liu, Q., Gui, D., et al. (2024). Precise vegetation restoration in arid regions based on potential natural vegetation and potential normalized difference vegetation index. *Restoration Ecology*, 32(2), e13967.
50. Reichstein, M., et al. (2013). Climate extremes and the carbon cycle. *Nature*, 500, 287–295.
51. Rouse, J. W., et al. (1973). Monitoring vegetation systems. NASA SP-351.
52. Sala, E., et al. (2001). Rapid decline of Nassau grouper spawning aggregations in Belize: fishery management and conservation needs. *Fisheries*, 26(10), 23–30.
53. Sarikaya, A. G., Orucu, O. K. (2021). MaxEnt modeling for predicting the potential distribution of *Arbutus andrachne* L. belonging to climate change in Turkey.. *Kuwait Journal of Science*, 48(2).
54. Sims, D. A., Gamon, J. A. (2003). Estimation of vegetation water content and photosynthetic tissue area from spectral reflectance: a comparison of indices based on liquid water and chlorophyll absorption features. *Remote Sensing of Environment*, 84(4), 526–537.
55. Singh, R. P., Roy, S., Kogan, F. (2003). Vegetation and temperature condition indices from NOAA AVHRR data for drought monitoring over India. *International Journal of Remote Sensing*, 24, 4393–4402.
56. Sun, G.-Q., et al. 2022. Impacts of climate change on vegetation pattern: Mathematical modeling and data analysis. *Physics of Life Reviews*, 43, 239–270.
57. Tarkesh, M., Jetschke, G. (2012). Comparison of six correlative models in predictive vegetation mapping on a local scale. *Environmental and Ecological Statistics*, 19, 437–457.
58. Trambly, Y., et al. (2012). Climate change impacts on extreme precipitation in Morocco. *Global and Planetary Change*, 82, 104–114.
59. Tucker, C. J. (1979). Red and photographic infrared linear combinations for monitoring vegetation. *Remote Sensing of Environment*, 8(2), 127–150.
60. Xu, H. (2006). Modification of normalised difference water index (NDWI) to enhance open water features in remotely sensed imagery. *International Journal of Remote Sensing*, 27(14), 3025–3033.
61. Xu, K., Wang, X., Jiang, C., Sun, O. J. (2020). Assessing the vulnerability of ecosystems to climate change based on climate exposure, vegetation stability and productivity. *Forest Ecosystems*, 7, 1–12
62. Zhang, Y., Li, M. L. (2025). Short-term load forecasting in power systems based on the Prophet–BO–XGBoost model. *Energies*, 18(2), 227.
63. Zhou, W., et al. (2014). Dynamic of grassland vegetation degradation and its quantitative assessment in the northwest China. *Acta Oecologica*, 55, 86–96.
64. Zribi, M., Dechambre, M. (2003). A new empirical model to retrieve soil moisture and roughness from C-band radar data. *Remote Sensing of Environment*, 84(1), 42–52.